Journal of the European Ceramic Society **19** (1999) 2701–2709

PII: S0955-2219(99)00051-5
0955-2219/99/$ - see front matter

$\beta \Rightarrow \alpha$ Phase Transformation in SiC: Link between Polytypism, Dihedral Angle and Nucleation Mechanism of α Twins

C. Ragaru, M. Lancin* and C. Marhic

CMC, Laboratoire de Physique Cristalline, Institut des Matériaux de Nantes, B.P. 32229 44322 Nantes Cedex 3, France

(Received 31 December 1998; accepted 21 February 1999)

Abstract

This paper deals with the $\beta \Rightarrow \alpha$ *phase transformation in SiC. The mechanism is studied in materials in which the transformation results in* α *twins, called feathers. The dihedral angle (*2α*) between the basal planes of the twin grains is related to the mean polytype of the feathers. The 15R polytype is predominant (about 67%) in the studied materials. An analysis of the 15R diffraction pattern shows that four different stackings could be expected in 15R feathers. The stacking in both branches of 15R feathers is studied by electron diffraction and HRTEM. Only one out of the four stackings expected is observed when* 2α *is large and two when* 2α *is small. Based on this result and on the symmetry elements of feathers whatever their mean polytype is, a discussion of the nucleation mechanism is developed.* © *1999 Elsevier Science Limited. All rights reserved*

Keywords: phase transformations, polytypism, electron microscopy, microstructure-final, SiC.

1 Introduction

Owing to its hardness and stiffness at high temperature and its large band gap, SiC is a good candidate to realise structural components and electronic devices. Moissanite, the natural substance, being extremely rare,[1] SiC must be synthesised and processed. SiC crystallises in numerous polymorphic structures called polytypes which are always categorised into two phases. The zinc-blende structure is called β phase and all the other hexagonal or rhombohedral polymorphs α phase. The temperature range of the β and α phases depends on numerous parameters such as temperature, pressure, impurities, reaction rate, substrate.[1–14] The fabrication of materials composed of a well defined polytype is thus, extremely difficult but it should be achieved in order to control their physical properties. As an example, a homogeneous microstructure is not obtainable by sintering of β-SiC powder because of a $\beta \Rightarrow \alpha$ phase transformation which results in large α grains ($> 100\,\mu$m) embedded in a matrix of small β grains ($< 10\,\mu$m). Such an heterogeneous microstructure is detrimental to the mechanical properties of the material. The control and thus, the understanding of the phase transformation in SiC appears to be necessary. This paper deals with the $\beta \Rightarrow \alpha$, phase transformation.

Several phase transformation mechanisms have been proposed in SiC. The $\beta \Rightarrow \alpha$ phase transformation results in α plates.[5,7–11] or α feathers[5,10,15,16] There is no typical orientation relationship between α plates. On the contrary, feathers consist of twin grains with well defined orientation relationships.[15,16] All the transformation mechanisms proposed involve dislocation glide but the driving force is either the decrease of the free energy or a mechanical stress.

The model proposed by Ogbuji *et al.*[9] was designed to explain α plate formation during the sintering of β SiC The phase transformation involves three successive mechanisms. First, α seeds nucleate from $\{112\}\Sigma = 3$ twin boundaries. Such twins are formed in cubic grains during the recrystallisation in epitaxy of β_e variants on $\{111\}$ planes. The twin boundary is described as a pile up of triplets of Shockley partial dislocations, the total Burger vector of which is equal to zero. According to the model, successive triplets glide alternately on either side of the boundary resulting in a 6H seed. The decrease of the free energy is the driving force

*To whom correspondence should be addressed.

for the motion of the partial dislocations. In the second stage of α plate formation, the recrystallisation of β_e variants on the α seed, is due to the lower β_e/β interfacial energy compared to the α/β interfacial energy.[8] In the last stage of the α plate growth, the $\beta_e \Rightarrow \alpha$ phase transformation is due to the glide of Shockley partial dislocations, the driving force resulting again from the difference of free energy between the β phase and the α polytype locally the most stable. According to the authors, the sluggishness of this stage of the transformation must be due to the difficult nucleation of partial dislocations in almost every layer of the β phase to be transformed. This model does not explain faster plate growth than β.

Pirouz proposed an alternative model for polytypic transformations which was first designed to describe twinning in semiconductors such as silicon.[17] This model, which involves the activation of a Frank-Read source, is based on the different mobilities of 30° Shockley partial dislocations. The leading partial may glide in a {111} primary glide plane whereas the trailing partial remains almost immobile. A faulted loop is formed by the leading partial, provided the resolved shear stress on the glide plane is high enough to overcome the resulting stacking fault, the line tension force of the dislocation and a back-stress (σ_{bs}) produced on the source by the surrounding faulted loops previously created. As a consequence, dislocation loops glide on n successive planes out of m, with the n/m ratio and thus the resulting polytype depending on the balance between local stresses. Such a mechanism is supported by ambiguous experimental evidence[18] but it could explain the rapid growth of *a* plates.

Based on a twin boundary study, a model[19] was proposed for the $\beta \Rightarrow \alpha$ phase transformation resulting in α feather formation. Feather boundary can be described as a periodic array of Shockley partial dislocations. The dislocations are supposed to glide on two sets of {111} planes located either in one cubic grain or in two $\Sigma = 3$ twin grains. Such a model explains the value of the high dihedral angles found in this study but clarifies neither the nucleation of the partials nor the driving force for the motion.

More generally, none of the above models explain why α plates or α feathers are formed during sintering. In order to better understand the $\beta \Rightarrow \alpha$ polytypic transformation in SiC, we found necessary to develop a new approach. This paper deals with phase transformation resulting in α twin growth. We study the relationship between polytypism and dihedral angles. We develop an analysis of the 15R stacking in the twins as a function of their dihedral angle. Based on these results, the different possible nucleation mechanisms are discussed.

2 Materials and Techniques

Materials known to contain feathers were selected.[15,16] They were obtained by hot-pressing or pressureless sintering of β SiC powder (0·3 μm) containing about 1·5% free carbon and 0·5% boron. Hot-pressing was performed under a uniaxial stress of 12·6 MPa, for either ten minutes at 2060°C (material A) or 1 h at 2150°C (material B). Materials A and B contain about 77 and 87% of α phase respectively. Material C was obtained by pressureless sintering of similar greens at 2060°C for 30 min and subsequent annealing at 2150°C for 1 h; it contained about 80% of α phase.

Thin films were prepared by mechanical grinding and ion thinning (Balzers). Conventional transmission electron microscopy (bright field and electron diffraction) was performed at 300 keV with a Philips CM30 twin microscope. High resolution transmission electron microscopy images (HRTEM), obtained at 300 keV with a Hitachi H9000NAR microscope (Scherzer resolution = 1·7Å) were digitized and processed using Semper software (Oxford Instruments). HRTEM images obtained at 200 keV with a Hitachi HF2000 FEG microscope (Scherzer resolution = 2·6 Å) were directly acquired with a Gatan CCD camera.

3 Results

3.1 Microstructural features of the materials

In all three materials, A, B and C, the microstructural features were not influenced by the processing. A study of the polytypism by electron diffraction shows that the phase transformation results in α twins, called feathers. The feather characteristics are in good agreement with previous results.[15,16] As shown by Fig. 1, α twin growth is much quicker than β grain growth. Figure 1 also shows the symmetrical and asymmetrical parts of the boundary, characteristic of transformation twins. As previously published, the twin grains share a $[11\bar{2}0]$ axis and they are composed of the same mean polytype, despite the microsyntaxy characteristic of SiC. The feathers are thus categorised according to their mean structure and their dihedral angle, 2α. This angle which is measured on $[11\bar{2}0]$ diffraction patterns, is known within $\pm 0{\cdot}3°$. As shown in Table 1, the predominant structure is most often 15R, sometimes 6H, rarely 4H. In some grains of a more complex structure, it is sometimes possible to identify two or three of these polytypes.

Two main conclusions can be deduced from the results in Tables 1 and 2. First, it is clear that small dihedral angles are twice as probable as large ones. Second, there is a link between polytype and

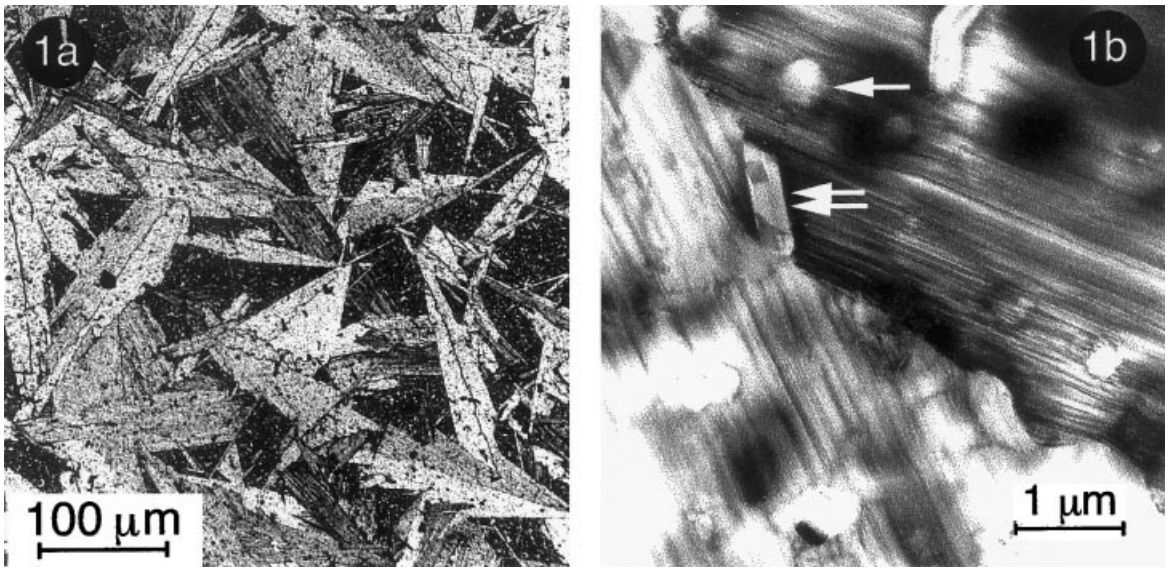

Fig. 1. Typical microstructure of the sintered materials. (a) Optical micrograph showing large α feathers and small β grains; (b) bright field TEM image of a feather: its irregular boundary follows as a mean the bisecting plane of the dihedral angle between the basal faces; graphite platelets (double arrows) and round shaped boron carbide (single arrow) grains are observed in α grains or in the boundary.

Table 1. In A and B hot pressed materials, results being similar are summarised in the same table.

Hot-pressed	*15R*	*6H*	*4H*	*6H+15R+..*	*4H+15R+..*	*Mixture*	*Total*
$2\alpha = 41°4$[a]	39	10		11	5	7	72
$2\alpha = 65°5$	39			1		1	41
$2\alpha = 64°5$		1					1
$2\alpha = 64°$			2				2
Total	78	11	2	12	5	8	116

[a]The feathers are categorised as a function of their mean polytype and of the dihedral angle 2α between their basal planes.

Table 2. Feathers in C materials as a function of the mean polytpe and dihedral angle 2α

Pressureless	*15R*	*6H*	*4H*	*6H+15R+.*	*4H+15R+.*	*Mixture*	*Total*
$2\alpha = 41°4$	13	3		2		2	20
$2\alpha = 65°5$	4						4
$2\alpha = 64°5$					1		1
Total	17	3		2	1	2	25

dihedral angle. Indeed, the 15R polytype is predominant in the large angle feathers with only few exceptions whereas only about 56% of the small angle feathers exhibit this structure. The 6H structure can be clearly identified together with the 15R one, and sometimes can be the predominant polytype, in a rather large proportion (about 30%) of small angle feathers.

The link between polytype and dihedral angle is confirmed by the few new feathers identified during this work. As for the small dihedral angles, some 4H feathers are detected but they contain a large proportion of other polytypes such as 15R (Fig. 2(a)). Note that 2α is equal to 41°4, a value which is thus typical of all small angle feathers whatever their structure. As for the large dihedral angles, the new feathers exhibit both a mean polytype and a 2α value different from those of typical 15R feathers. In the two 4H feathers, 2α is equal to 64° such as in the only 4H feather previously identified,[15] but, a large amount of stacking faults in a 4H structure increases the 2α value from 64° to 64°5, that means beyond the experimental error. In the only 6H feather identified, 2α is equal to 64·5° (Fig. 2(b)) but it reaches its usual value, 65·5°, when the 6H grains contain a large amount of 15R polytype. The dihedral angle is thus related to the mean grain structure. The link between polytype and dihedral angle could result from the nucleation mechanism. To better explicit this link, the stacking in 15R twin grains is characterised in the next section.

3.2 15R stacking in twin grains

In a 15R grain, the orientation of the [0001] axis being chosen, the stacking of the basal planes can be ABCACB (Fig. 3(a)), designated type (1) or ABCBAC (Fig. 3(c)), designated type (2). Let us now consider a feather projection along the [11$\bar{2}$0] axis with the apex of the dihedral angle located on the upper part of the figure and the boundary

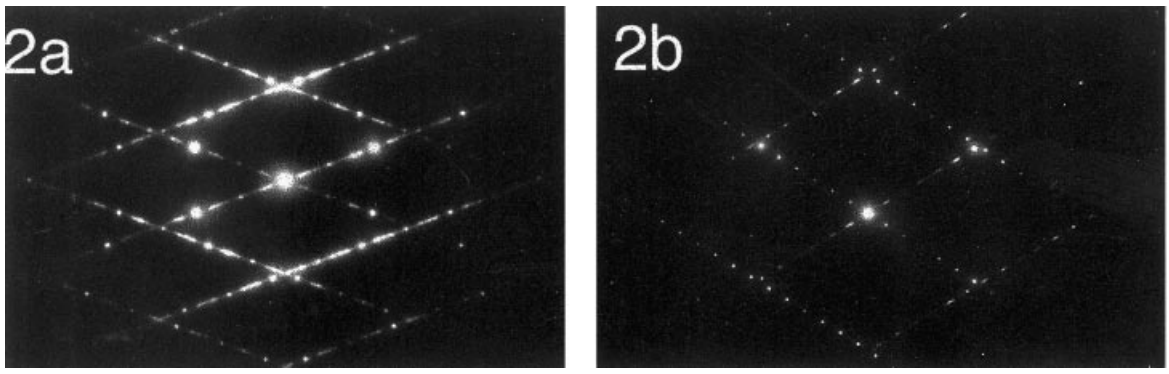

Fig. 2. Diffraction pattern of newly identified feathers. (a) 4H feather: 2α, the dihedral angle between the (0001) planes is equal to 41°4; both twin grains contain numerous stacking faults (b) 6H feather: $2\alpha = 64°$.

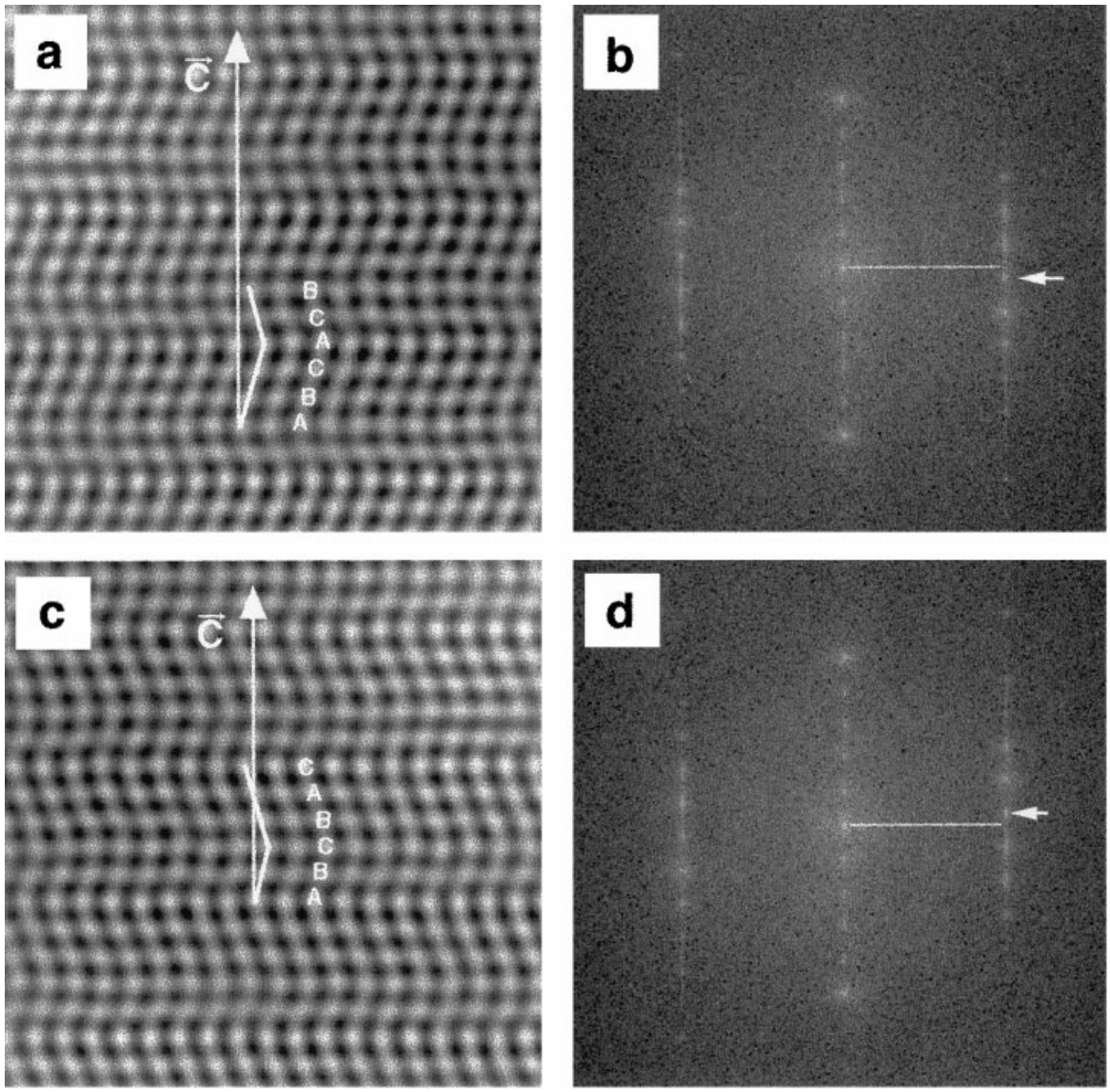

Fig. 3. The two possible types of 15R stacking. The orientation of the C axis being known, the 15R structure is obtained by two different stackings designed (1) and (2). Figure 3(a) and (c) are obtained by simulation of the contrast of the (1) and (2) stackings respectively. In these images viewed along the [11$\bar{2}$0] axis, each white dot corresponds to the projection of one Si and one C atomic column (SiC dumbbells) in the (11$\bar{2}$0) plane. Figure 3(b) and (d) show the power spectrum of Fig. 3(a) and (c) images respectively. The white lines and arrows underline the asymmetry of the 15R diffraction patterns.

running from top to bottom. We call L and R the grains located on the left and on the right hand side of the boundary respectively. The C axes are directed from the boundary towards the external faces of the twin grains. Due to the possible stackings in each grain, four distinct feather structures are expected, namely L1R1, L1R2, L2R1 and L2R2. The relative amounts of these different stackings are measured in large and small angle feathers.

HRTEM images reveal the twin grain stacking but only in a small percentage of the feathers because of experimental requirements. Concerning the 15R feathers, the stacking can be derived from the asymmetry of the $[11\bar{2}0]$ diffraction patterns (Fig. 3(b) and (d)). The orientation of the C axes being imposed as described above, the experimental pattern of each twin grain is compared with standards to deduce the grain stacking and therefore the kind of feather. Figure 4 shows a typical large angle feather. The diffraction pattern (4(a)) reveals type (1) and type (2) stacking in the left and right grains respectively. Therefore, the feather belongs to the L1R2 kind. The HRTEM image (4(b)) shows the L1 and R2 stacking as well as the stacking faults characteristic of SiC. The L1R2 stacking is the only one identified in all the large angle feathers which could be analysed in hot pressed and pressureless materials (Table 3).

In small angle feathers, on the contrary, two possible stackings, L1R2 and L2R1, are observed. The diffraction patterns and the HRTEM images of the two stackings are imaged in Fig. 5. According to the results shown in Table 3, the two stackings occur with the same probability in hot pressed materials. A similar conclusion seems to be valid in the pressureless material.

3.3 Inclusions

To achieve sufficient densification, the greens contain additives, boron and carbon powder, which react with the β-SiC powder and form graphite and boron carbide inclusions.[20,21] We investigate if any of their faces could act as nucleation site of the feathers. The feathers contain numerous inclusions located either in the twin grains or at the twin boundary (Fig. 1(b)). Graphite inclusions form typical platelets with {0001} faces and round shaped ends. From 500 nm to 2 μm long, they generally have no particular orientation relationship with the surrounding grains. A few are in epitaxy with the surrounding α grain, $\{0001\}_g // \{0001\}_\alpha$. Numerous graphite inclusions are located along the twin boundary. In such a case, the $\{0001\}g$ plane is sometimes parallel to the mean twin boundary plane but the graphite/α interfaces do not run along any particular reticular plane. The boron carbide grains range from 200 nm to one micron in size. Rather round shaped, they exhibit no particular orientation relationships with the surrounding α grains.

4 Discussion

The results described in this paper confirm and complete those previously published on similar

Table 3. 15R stacking in small and large dihedral angle feathers

	Small HP	*Angle PS*	*Total*	*Large HP*	*Angle PS*	*Total*
L1R2	13	7	20	18	4	22
L2R1	13	6	19			
Total	26	13	39	18	4	22

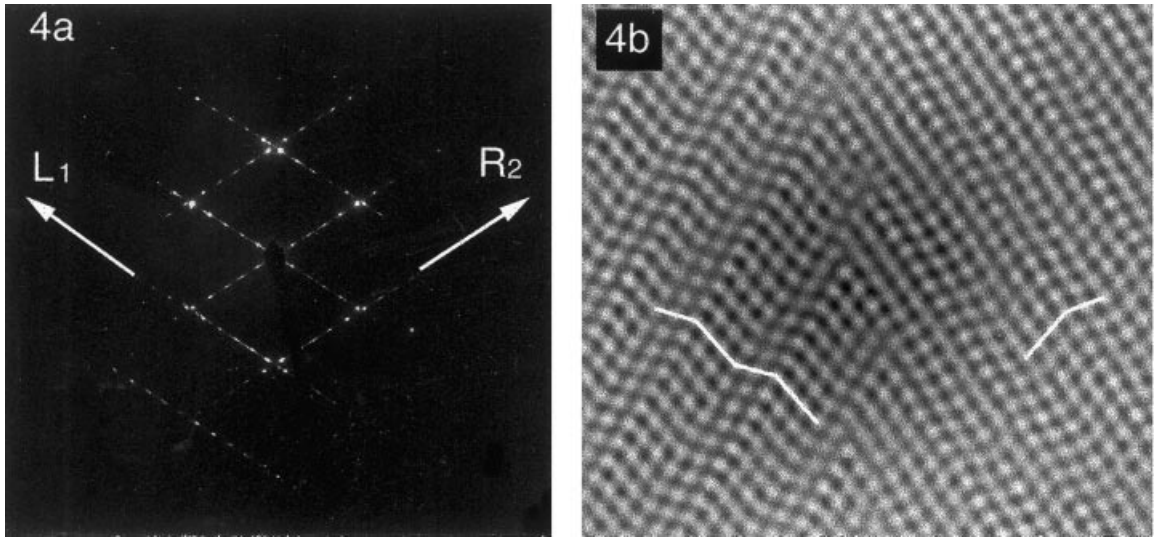

Fig. 4. 15R stacking in large angle feathers. The 15R feather is viewed along the $[11\bar{2}0]$ axis (300 keV, black atoms). In 4(a) diffraction pattern showing the (1) and (2) stacking in the left (L) and right (R) grains; L1R2 is the only stacking detected in large angle feathers. In 4(b) HRTEM image showing the L1R2 stacking, as well as stacking faults.

materials and we now have reliable statistics on their microstructural features. The 15R polytype is the most stable structure (67%) after natural sintering or hot-pressing of β-SiC with boron and carbon additives at high temperature ($>2000°C$). This result is in reasonable agreement with that of Williams obtained under similar conditions.[11] When the $\beta \Rightarrow \alpha$ phase transformation is almost completed, most of the α phase forms feathers, small dihedral angles being twice as probable as the large ones. Study of the twin grain structure suggests that polytype and dihedral angle are related. The analysis of the 15R stacking described in this paper confirms this hypothesis. The feather formation must explain this link, and particularly why L2R1 stacking has not been detected in large angle feathers and why L1R1 and L2R2 stackings are never observed whatever the dihedral angle.

The analysis of the orientation relationships and the irregularity of the boundaries have shown that feathers are transformation twins.[15,16] The same analysis can be performed for the feathers newly identified. Among the symmetry elements of such twins, two, K_1, and η_1, are of major importance in considering the nucleation mechanism. K_1, is the mirror plane of the twin grains and η_1 the trace of K_1, in the common $(11\bar{2}0)$ plane (Fig. 6). Their indices in the 6H (64°5) feather are, $\eta_1 = [9\bar{9}02]$ and $K_1 = (\bar{1}109)$ and in 4H (41°4) feathers $\eta_1 = [5\bar{5}01]$ and $K_1 = (\bar{1}1010)$. As is well known, transformation twin formation involves two distinct mechanisms, nucleation and growth. The nucleation mechanism determines the orientation relationships between the twin grains and, therefore, this mechanism must explain the observed link between polytype and dihedral angle.

We first determine if twin nucleation occurs after the phase transformation or results from it. When a twinning occurs in the α phase, one of the two following mechanisms is generally involved. In the

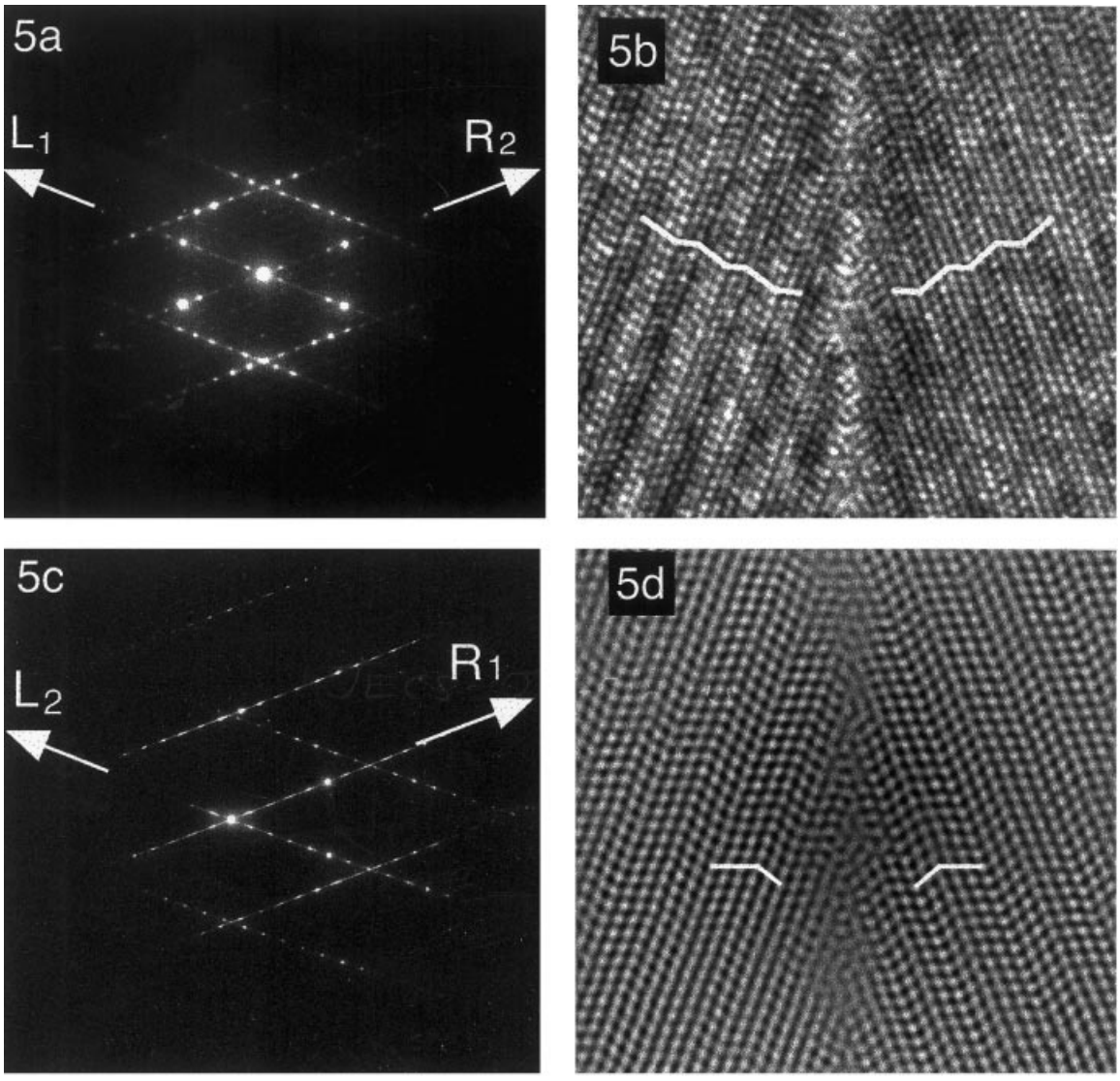

Fig. 5. 15R stacking in small angle feathers. The 15R feather is viewed along the $[11\bar{2}0]$ axis. Two kinds of stacking are observed in small angle feathers. L1R2 stacking: 5(a) diffraction pattern and 5(b) HRTEM image (200 keV, white atoms); L2R1 stacking: 5(c) diffraction pattern and 5(d) HRTEM image (300 keV, white atoms).

first, nucleation results from α stacking fault in an α grain during its growth. In this case, the K_1, plane, which is the mean twin boundary plane, is the growth facet. Whatever the feather structure, the K_1, plane always has very high indices (see above or K_1 indices in the 15R feathers [$(\bar{1}1038)$ or $(\bar{1}1022)$].[15,16] Such growth facets have never been identified in hexagonal or rhombohedral structures and it is not reasonable to believe that preferential growth occurs in planes of such high indices. The second mechanism was proposed because transformation twins are basically mechanical in nature[22].

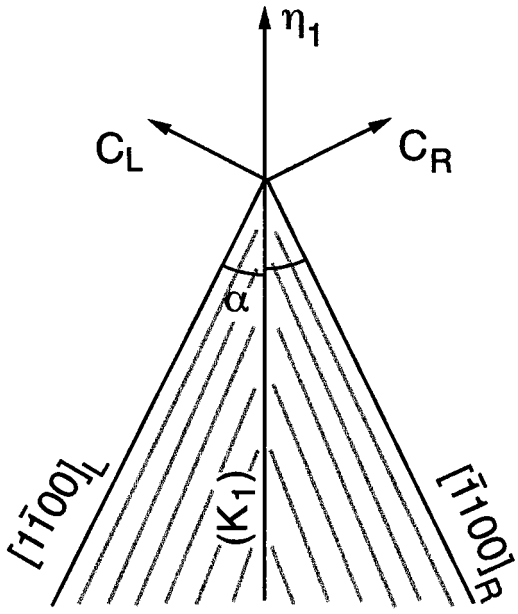

Fig. 6. Schematic of the symmetry elements in a feather viewed along the $[11\bar{2}0]$ axis. The drawing shows the traces of the basal planes, the dihedral angle 2α, the C axis of the L and R twin grains, the mirror plane K_1, and the symmetry axis η_1.

In such a model, twinning occurs by homogeneous shearing of part of an α crystal in the η_1 direction parallel to the K_1 plane. Again, because of the high indices of η_1 and K_1, this mechanism cannot be involved in feather nucleation. Twinning could also occur in the α phase if inclusions could act as nucleation sites. Such a hypothesis is not supported by experimental evidence because suitable orientation relationships between α grains and inclusions have never been observed.

In conclusion, feather nucleation must occur in the β phase and results in the $\beta \Rightarrow \alpha$ phase transformation, and, because the dihedral angles are not characteristic of the cubic phase, nucleation must involve dislocation glide. We previously supposed that the feathers could nucleate by glide of Shockley partials on two sets of {111} planes in cubic grains or $\{112\}\Sigma = 3$ twins.[19] We first discuss if such a hypothesis can result in the different 15R stacking and dihedral angles observed and, then, the possible origin of these dislocations.

The cubic grains or $\{112\}\Sigma = 3$ twin in which large angle or small angle feathers will nucleate are imaged in Fig. 7(a) and (b) respectively. A comparison between Figs 7(a) and 4(b) on one hand and between Figs 7(b) and 5(b) or Fig. 5(d) on the other shows the following. The L1R2 stacking characteristic of large angle feathers could be obtained by shearing two out of five successive {111} planes. The L1R2 and the L2R1 stackings observed in the small angle feathers could result from the shearing of three or two {111} planes out of five respectively. In a feather seed, the boundary must be the mirror plane of the twin grains, that is to say must be the K_1 plane. If the hypothesis is

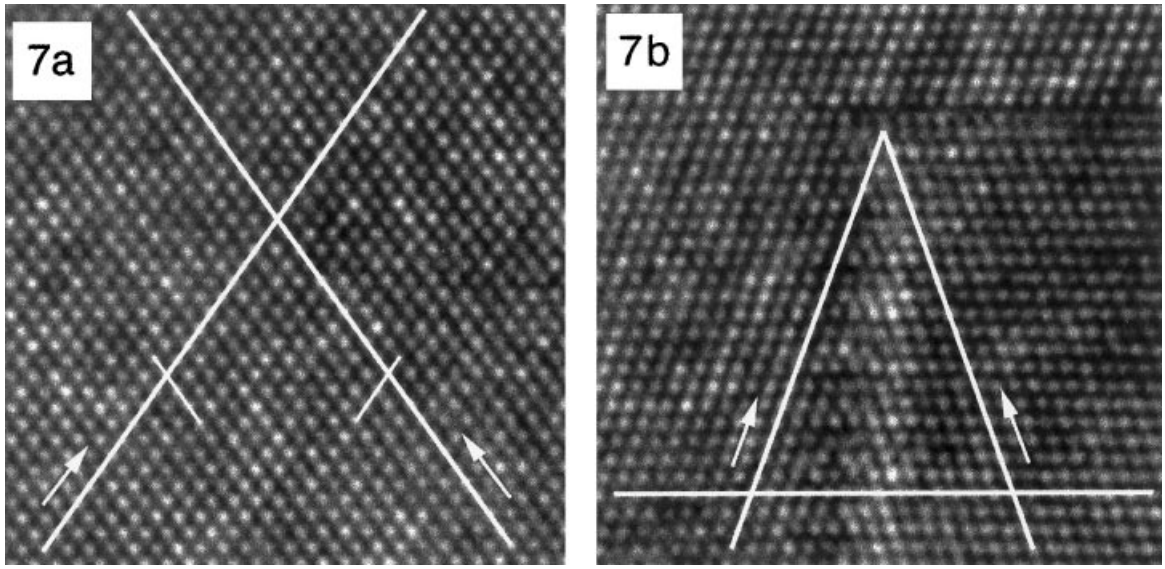

Fig. 7. HRTEM of a cubic grain and of a $\{112\}\Sigma = 3$ twin. In the HRTEM images (200 keV) viewed along a $<110>$ axis, SiC dumbbells are black. According to the nucleation mechanism, 30° Shockley partial dislocation glide in n {111} planes out of m. The traces of a glide plane are drawn and arrowed on the images of a cubic grain 7(a) and of a $\{112\}\Sigma = 3$ twin 7(b). The traces of the planes which will be sheared are also drawn.

verified, coincidence sites must be found every five planes in the K_1 plane, along the η_1 direction. A reconstruction of the boundary structure is out of the scope of this work, however, on a projection along the [11$\bar{2}$0] direction of the different stackings, it is possible to verify if such a periodic coincidence is possible. As shown in Fig. 8((a),(d) and (c)), the L1R2 and L2R1 stackings in small angle feathers and the L1R2 stacking in large angle feathers lead to the coincidence sites expected according to the model. Therefore, the feather nucleation may be due to a periodic shearing of {111} planes in cubic grains or $\{112\}\Sigma = 3$ twins. However, as far as lattice symmetry is concerned, other shearing process that those observed are also possible. As an example, nothing prevents shearing of three planes out of five in a cubic grain, resulting in a mirror plane where coincidence sites occur every five {111} planes (Fig. 8d). If such a shearing did occur, K_1, and η_1, would have different indices than in the L1R2 stacking and the dihedral angle would be equal to 63°, a value which has never been found. In the same way, coincidence sites could be obtained with L1R1 or L2R2 stackings which never occur. A discussion of the origin of the dislocations involved in the shearing must explain why these three stackings are never observed.

Numerous fronts of Shockley partial dislocations observed in β-SiC grains[23,25] are created to release internal stresses due to impurity gradients or/and to decrease the free energy of the crystal by phase transformation. The resultant total Burgers vector of these fronts is either equal to zero when $3n$ planes are sheared (n integer) or to $1/12 < 112 > a_c$, (a_c = lattice parameter of the β cell) when $3n+1$ or $3n+2$ planes are sheared. The glide of these fronts results in highly faulted β-SiC but does not induce any long range order. Moreover, the intersection of such fronts can result neither in the twin angles nor in the dislocation network observed in a 15R twin boundary and therefore it cannot result in a feather seed. For the same reasons, the Ogbudji *et al.* model[9] cannot explain the feather nucleation.

The partial dislocations responsible for the phase transformation could be created by a Frank-Read source as proposed by Pirouz *et al.*[17] In order to obtain feathers, two sources located in two sets of {111} planes must be involved. Such a model may explain some characteristics of the feathers. First, the projection in the glide plane of the resultant Burgers vector of two successive 30° Shockley partial dislocations is equal to $1/6 < 112 > a_c$, in good agreement with the value found in one 15R twin boundary.[19] Second, the model can explain the different feather stackings as well as the numerous stacking faults. Local variation of the resolved shear stress on the glide plane modifies the number

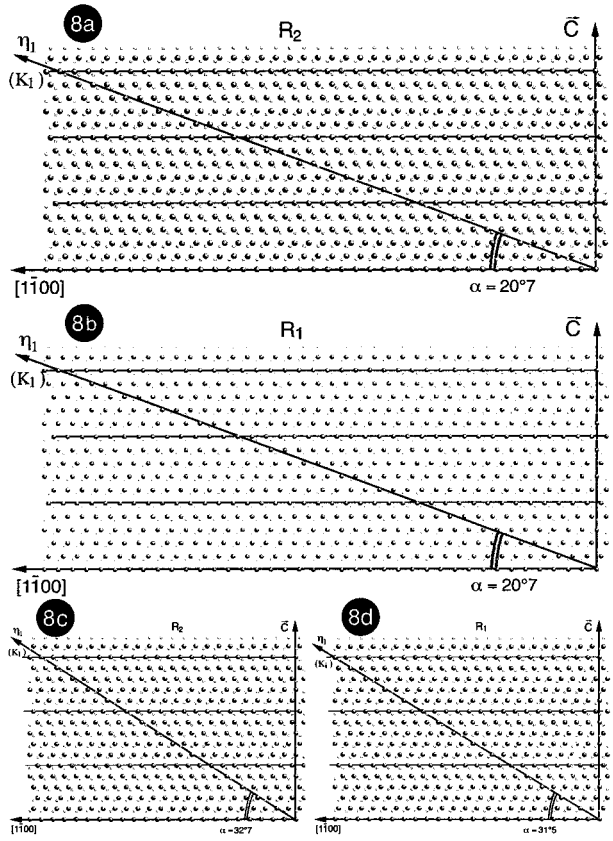

Fig. 8. Projection along [11$\bar{2}$0] axis of the atomic structure of 15R grains and of the symmetry elements. The large and small circles correspond to the projections of Si and C atomic columns respectively. The C axis, the trace of the K_1, plane, the η_1, direction and the dihedral angle are drawn. 8(a) Projection of a right grain (R) characterised by a (2) stacking in L1R2 small angle feathers; 8(b) Projection of a R1 grain in L2R1 small angle feathers; 8(c) Projection of a R2 grain such as in all L1R2 large angle feathers; 8(d) Projection of a R1 grain which has never be detected in a large angle feathers.

n of plans sheared out of m. Last, the greater is the dihedral angle the smaller is the Schmidt factor and thus, the smaller is the stress which counterbalances the line tension force, the stress due to the stacking fault and the back stress. As a consequence, small angle feathers should be more probable than large angle. In addition, shearing of three planes out of five should be more probable in small angle feathers than in large ones, just as is observed experimentally. However, several requirements must be fulfilled for the Pirouz model to apply. The more restrictive concern (i) the Burgers vector of the two sources, which must explain the stacking and the dihedral angle, (ii) the different mobilities of the partials, which is not straightforward at such high temperatures and (iii) the probability to activate two sources simultaneously, that is to say to nucleate α feathers rather than α plates. Studies of the grain boundary structure[24] and of the growth mechanism will provide useful arguments to discuss this model.

5 Conclusion

A $\beta \Rightarrow \alpha$ phase transformation occurs during the processing or subsequent anneals when β-SiC is sintered at high temperature ($>2000°C$) with boron and carbon additives. With such experimental conditions, the 15R polytype is the most stable. When the transformation is almost completed, most of the α phase forms twins, called feathers, characterised by their mean polytype and the dihedral angle between the basal planes of the twin grains. A study of the twin grain structure suggests that polytype and dihedral angle are related. The determination of the stacking in both branches of 15R feathers confirms this conclusion.

An analysis of their symmetry elements shows that feathers cannot nucleate in α grains during their growth. Their nucleation which results from the $\beta \Rightarrow \alpha$ phase transformation must involve dislocation glide. The transformation may proceed by shearing n {111} planes out of m in cubic grains or in {112} $\Sigma = 3$ twin grains. The 15R stacking observed in the twin grains supports such an hypothesis. A discussion of the shear mechanism shows that Pirouz's model proposed for the $\beta \Rightarrow \alpha$ phase transformation may be involved in the feather nucleation. Such a model may explain how different polytypes can be obtained, the stacking faults and the different stackings in feathers exhibiting large or small angle dihedral angle. However, this model implies severe requirements which are under study.

Acknowledgements

The authors thank Jean Charles Ricquier for the drawings.

References

1. Knippenberg, W. F., *Philips Res. Repts*, 1963, **18**, 161–274.
2. More, K. L., Ryu, J., Carter, C. H., Bentley, Jr. J. and Davis, R. F., *Adv. in Ceram*, 1987, **23**, 477–504.
3. Shaffer, P. T. B., *Acta Cryst*., 1969, **B25**, 477–488.
4. Vodokov, Yu. A., Mokhov, E. N., Roenkov, A. D. and Saidbekov, D. T., *Phys. Stat. Sol. (a)*, 1979, **51**, 209–215.
5. Johnson, C. A. and Prochazka, S., *Ceramic Microstructures*, Ed. R. Fulreth and J. A. Pask. Westview Press, 1977, pp. 366–377.
6. Lange, F. F. and Gupta, T. K., *J. Am. Ceram. Soc.* 1976, **59**, (11–12), 537–538.
7. Kinsman, K. R. and Shinozaki, S., *Scripta Metallurgica*, 1978, **12**, 517–523.
8. Mitchell, T. E., Ogbuji, L. U. and Heuer, A. H., *J. Am. Ceram. Soc*., 1978, **61**(9–10), 412–413.
9. Ogbuji, L. U., Mitchell, T. E. and Heuer, A. H., *J. Am. Ceram. Soc*., 1981, **64**(2), 91–99.
10. Ogbuji, L. U., Mitchell, T. E., Heuer, A. H. and Shinozaki, S., *J. Am. Ceram. Soc*., 1981, **64**(2), 100–105.
11. Williams. R. M., Juterbock, B. N., Peters, C. R. and Whalen, T. J., *Com. Am. Ceram. Soc*., 1984, **C-62-64**.
12. Jagodzinski, H., *Zeitschrift für Kristallographie*, 1995, **210**, 481–488.
13. Chaudhuri, J., Cheng, X., Yuan, C. and Steki, A. J., *Thin Solid Films*, 1997, **292**, 1–6.
14. Kimoto, T., Itoh, A. and Matsunami, H., *Physica Status Solidi B*, 1997, **202**(1), 247–262.
15. Lancin, M., *J. Mat. Sci*., 1984, **19**, 4077–4086.
16. Lancin, M., Anxionnaz, E., Thibault-Desseaux, J., Stutz, D. and Greil, P., *J. Mat. Sci*., 1987, **22**, 1150–1156.
17. Pirouz, P. and Yang, J. W., *Ultramicroscopy*, 1993, **51**, 189–214.
18. Pirouz, P., Yang, J. W., Powell, J. A. and Ernst, E., *Inst. Phys. Ser*. 1991, **117**, 149–154.
19. Lancin, M. and Thibault-Desseaux, J., *Journal de Physique C-5*, 1988, **49**(10), 305–309.
20. Prochazka, *Special Ceramics*, vol. ed. 6, P. Popper. Mac Corquodale Printers, 1975.
21. Bressiani, A. H. A., Ph.D. thesis, Stuttgart University, 1984.
22. Cahn, R. W., *Ad Phys. Suppl. Phil Mag*., 1954, **3**, 363–445.
23. Ragaru, C., Ph.D. thesis, Univ. Nantes, 1997.
24. Ragaru, C., Lancin, M. and Thibault, J. *Proc. of iib98,* Prague 6-9/07/1998, *Materials Science Forum*, Vols 294–296, 1999, pp. 285–288.
25. Godon, C., Ragaru, C., Hardouin Duparc, O. and Lancin, M., *Proc. of iib98,* Prague 6–9/07/1998, *Materials science Forum*, Vols 294–296, 1999, pp. 277–280.